RSC Advances

ROYAL SOCIETY OF CHEMISTRY

www.rsc.org/advances

Cite this: DOI: 10.1039/c0xx00000x

www.rsc.org/xxxxxx

ARTICLE TYPE

Substituent effect on fluorescence signaling of the cell permeable HSO_4^- receptors through single point to ratiometric response in green solvent†

Manjira Mukherjee,[a] Siddhartha Pal,[a] Buddhadeb Sen,[a] Somenath Lohar,[a] Samya Banerjee,[b] Snehasis Banerjee[c] and Pabitra Chattopadhyay[a]*

Received (in XXX, XXX) Xth XXXXXXXXX 20XX, Accepted Xth XXXXXXXXX 20XX
DOI: 10.1039/b000000x

Abstract

Two new *2-(2-aminophenyl)benzimidazol* based HSO_4^- ion selective receptors, *6-(4-nitro-phenyl)-5,6-dihydro-benzo[4,5]imidazo[1,2-c]quinazoline* (**L_1H**) and *6-(4-methoxy-phenyl)-5,6-dihydro-benzo[4,5]imidazo[1,2-c]quinazoline* (**L_2H**), and their 1:1 molecular complexes with HSO_4^- were prepared in a facile synthetic method and characterized by physico-chemico and spectroscopic tools along with the detailed structural analysis of **L_1H** by single crystal X-ray crystallography. Both receptors (**L_1H** and **L_2H**) behave as highly selective chemosensor for HSO_4^- ions at biological pH in ethanol-water HEPES buffer (1/5) (v/v) medium over other anions such as F^-, Cl^-, Br^-, I^-, AcO^-, $H_2PO_4^-$, N_3^- and ClO_4^- etc. Theoretical and experimental studies showed that the emission efficiency of the receptors (**L_1H** and **L_2H**) has been tuned successfully through single point to ratiometric detection by employing the substituent effects. Using 3σ method the LOD for HSO_4^- ions were found to be 18.08 nM and 14.11 nM for **L_1H** and **L_2H** respectively within a very short responsive time (15-20 s) in 100 mM HEPES buffer (ethanol/water:1/5, v/v). Comparison of the utility of the probes (**L_1H** and **L_2H**) as biomarkers for the detection of intracellular HSO_4^- ions concentrations under a fluorescence microscope has also been included and both probes showed no cytotoxic effect.

Introduction

The design and development of selective receptors for the anionic analytes have gained considerable attention in recent years because of the biological significance of the field, potential applications in sensors and the development of phase transfer reagents.[1,2] Critical physiological processes are being operated through negative ion gradients across lipid bilayer membranes originated by anion channels.[3] The malfunction of this process leads to severe diseases such as cystic fibrosis, nephrolithiasis, osteopetrosis, Angelman syndrome and Bartter's syndrome type III.[4] Among the various anions, hydrogen sulfate (HSO_4^-) ions dissociate at high pH to generate toxic sulfate (SO_4^{2-}), causing irritation of the skin and eyes and even respiratory paralysis.[5] Despite its crucial roles in biological processes, only few examples of cell permeable sensors for HSO_4^- have been reported.[6] So the design of anion sensors for the hydrogen sulfate ion is important and desirable.

Sensors based on anion-induced changes in fluorescence are particularly attractive due to the simplicity, high degree of specificity and low detection limits.[7] But from the experimental point of view, it is well known that the ratiometric responses are more attractive because the ratio between the two emission intensities can be used to measure the analyte concentration and provide a built-in correction for environmental effects and stability under illumination.[8] There are some reports either single point sensor or ratiometric response, but there is no report of tuning of single point to ratiometric response keeping the same receptor environment except the change in electronic effect using substituents.

Herein, two newly designed efficient HSO_4^- ion selective receptors, *6-(4-nitro-phenyl)-5,6-dihydro-benzo[4,5]imidazo-[1,2-c]quinazoline* (**L_1H**) and *6-(4-methoxy-phenyl)-5,6-dihydro-benzo[4,5]imidazo[1,2-c]quinazoline* (**L_2H**) from *2-(2-amino-phenyl)benzimidazol* (*viz*. **Scheme 1**) keeping same receptor environments for the guest (HSO_4^- ions) have been employed to tune the emission efficiency of these new receptors (**L_1H** and **L_2H**) through single point to ratiometric detection in green solvent by exploiting the effects of the substituents within the receptors. The organic moieties (**L_1H** and **L_2H**) and the resulting compounds (**K[L_1H-HSO_4]** and **K[L_2H-HSO_4]**) have been characterized by physico-chemico and spectroscopic tools along with the crystallographic analysis of **L_1H** by single crystal X-ray diffractometer. Both **L_1H** and **L_2H** behave as highly selective fluorescent and colorimetric sensor for HSO_4^- ions at biological pH in ethanol-water HEPES buffer (1/5) (v/v) medium over other anions such as F^-, Cl^-, Br^-, I^-, AcO^-, $H_2PO_4^-$, N_3^- and ClO_4^- etc. The receptor **L_1H** behaves as a single point fluorosensor whereas the receptor **L_2H** as a ratiometric fluorosensor in an identical

condition. Both the probes ($\mathbf{L_1H}$ and $\mathbf{L_2H}$) were also employed to detect the presence of intracellular bisulphate ions by acquiring the images of HeLa cells under a fluorescence microscope. Comparison of these acquired images showed that the image through ratiometric signaling using $\mathbf{L_2H}$ is better one for cell staining though both probes have no cytotoxic effect.

Experimental Section

Physical measurements

The fluorescence property of the sensor was investigated in water : ethanol (5 : 1, v/v) solvent. The pH study was done in 100 mM HEPES buffer solution by adjusting pH with HCl or NaOH. The stock solutions (~ 10^{-2} M) for the selectivity study of the receptors ($\mathbf{L_1H}$ and $\mathbf{L_2H}$) towards different anions were prepared taking sodium perchlorate, disodium hydrogen arsenate, tetra butyl ammonium salt of chloride, bromide, iodide, acetate, fluoride, dihydrogen phosphate and potassium hydrogen sulphate; in water : ethanol (5 : 1, v/v) solvent. In this selectivity study the amount of these anions was a hundred times greater than that of the receptor used. Fluorescence titration was performed with Potassium hydrogen sulphate in water: ethanol (5 : 1, v/v) solvent varying the anion concentration 0 to 100 μM and the receptor concentration was 25 μM.

Preparation of L_1H and L_2H

Preparation of two receptors $\mathbf{L_1H}$ and $\mathbf{L_2H}$ were carried out following a common procedure. *2-(2-aminophenyl)-benzimidazole* (2.09 g, 10.0 mmol) and *4-nitro benzaldehyde* (1.51 g, 10.0 mmol) (for $\mathbf{L_1H}$) or *4-methoxy benzaldehyde* (1.36 g, 10.0 mmol) (for $\mathbf{L_2H}$) were mixed in dry ethanol (25.0 mL) at room temperature. Then the reaction mixture was continued to reflux for 6.0 h. The yellow ($\mathbf{L_1H}$) or brown ($\mathbf{L_2H}$) precipitate of the compounds were obtained from the solution through slow evaporation of the solvent. The pure recrystallized compounds were isolated from the methanol.

L_1H. $C_{20}H_{14}N_4O_2$: Anal. Found: C, 70.49; H, 4.24; N, 16.51; Calc.: C, 70.17; H, 4.12; N, 16.37. IR(cm^{-1}) : ν_{NH} = 3190.26, $\nu_{C=N}$ = 1612.49; ESI-MS: $[M + H]^+$, m/z, 343.1480(100 %) (calcd.: m/z, 342.11; where M = molecular weight of $\mathbf{L_1H}$]; ^{1}HNMR (δ, ppm in dmso-d6): 8.201 (d-d, 2H, J_1=7, J_2=2); 7.986 (d-d, 1H, J_1 = 7.75, J_2=1.5); 7.8 (d, 1H, J=2.5); 7.7 (d, 1H, J = 8); 7.448(d-d, 2H, J_1 = 7, J_2=2); 7.361-7.337(m, 2H); 7.281-7.165(m, 3H); 6.884-6.856(m, 2H) Yield: 90%.

L_2H. $C_{21}H_{17}N_3O$: Anal. Found: C, 76.81; H, 5.15; N, 13.07; Calc.: C, 77.03; H, 5.24; N, 12.84. ESI-MS: $[M + H]^+$, m/z, 328.1246 (100 %) (calcd.: m/z, 328.14; where M = molecular weight of L2H]; IR(cm-1) : ν_{NH} =3209.6, $\nu_{C=N}$ = 1608.63 ^{1}H NMR (δ, ppm in dmso-d_6): 7.96 (d-d, 1H, J_1 = 7.6,J_2=2); 7.651 (d, 1H, J = 8); 7.307-7.077 (m, 7H); 6.866-6.734(m, 3H); 6.604(d-d, 1H, J_1 = 7.6,J_2=2); 4.401(s, 1H); 3.601(s,1H). Yield: 90%.

Preparation of compounds $K[L_1H\text{-}HSO_4]$ and $K[L_2H\text{-}HSO_4]$

The preparation of solid complexes was carried out following a common procedure.

To a methanolic solution of $\mathbf{L_1H}$ (342 mg, 1.0 mmol) or $\mathbf{L_2H}$ (327 mg, 1.0 mmol) (for $\mathbf{K[L_1H\text{-}HSO_4]}$) or for $\mathbf{K[L_2H\text{-}HSO_4]}$), solid potassium hydrogen sulphate (136 mg, 1.0 mmol) was added at a time and the reaction mixture was stirred at ambient temperature for 6.0 h. The solution thus obtained was then kept aside for slow evaporation at room temperature. After a few days, deep yellow crystalline complex were collected by washing with water and methanol, and then dried in vacuo.

$K[L_1H\text{-}HSO_4]$. $C_{20}H_{15}KN_4O_6S$: Anal. Found: C, 50.04; H, 3.25; N, 11.91; Calc.: C, 50.19; H, 3.16; N, 11.71. ESI-MS in methanol: $[I^{2-} + 2H + Na]^+$, m/z, 463.16 (obsd. with 6 % abundance) (calcd.: m/z, 463.06); $[I^{2-} + K + Na + H]$+, m/z, 505.0080 (obsd. with 12 % abundance) (calcd.: m/z, 505.06); where $I^{2-} = L_1+HSO_4^-$. IR(cm-1) : $\nu_{S=O}$ =1114.86; 1H NMR (δ, ppm in dmso-d6): 8.201 (d-d, 2H,J_1=7,J_2=2); 8.0 (d-d, 1H, J_1 = 7.75,J_2=1.5); 7.82 (d, 1H,J=2.5); 7.72 (d, 1H, J = 7.5); 7.480-7.458(m, 2H); 7.39-7.175(m, 5H); 6.906–6.875(m, 2H). Yield: 75 %.

$K[L_2H\text{-}HSO_4]$. $C_{21}H_{18}KN_3O_5S$: Anal. Found: C, 54.15; H, 3.99; N, 9.25; Calc.: C, 54.41; H, 3.92; N, 9.07. ESI-MS in methanol: $[I^{2-} + 2H + Na]^+$, m/z, 447.92(obsd. with 11 % abundance) (calcd.: m/z, 448.089); $[I^{2-} + K + Na + H]^+$, m/z, 486.2086 (obsd. with 35 % abundance) (calcd.: m/z, 486.09; where $I^{2-} = L_2+HSO_4^-$;IR(cm-1) : $\nu_{S=O}$ = 1111.00, ^{1}H NMR (δ, ppm in dmso-d6): 7.96 (d-d, 1H, J_1 = 7.6,J_2=2); 7.645 (d, 1H, J = 8); 7.306-7.077 (m, 7H); 6.867-6.731(m, 3H); 6.65(d-d, 1H, J_1 = 7.6,J_2=1.6); 4.401(s, 1H); 3.601(s,1H).Yield: 75 %.

X-ray data collection and structural determination

Single crystals suitable for single crystal X-ray crystallography were obtained from the methanolic solution of of $\mathbf{L_1H}$ on slow evaporation at room temperature. X-ray single crystal data were collected using Mo-K_α (λ = 0.7107 Å) radiation on a SMART APEX II diffractometer equipped with CCD area detector. Data collection, data reduction, structure solution/refinement were carried out using the software package of SMART APEX II. Crystallographic data and selected bond lengths and bond angles are tabulated in **Table 1** and **2**. A total of 26495 reflections were measured out of which 3542 were independent and 3202 were observed [I>2 σ(I)]. The structure was solved by direct methods using SHELXS-97[9] and refined by full-matrix least squares refinement methods based on F^2, using SHELXL-97. All non-hydrogen atoms were refined anisotropically. All calculations were performed using Wingxpackage.[10] Important crystal and refinement parameters are given in **Table 1**. The crystals that resulted were found suitable for structural studies.

Preparation of cell and *in vitro* cellular imaging

Human cervical cancer cell, HeLa cell line was used throughout the study. Cell were cultured in Dulbecco's modified Eagle's medium (DMEM, Gibco BRL) supplemented with 10% FBS (Gibco BRL), and 1% antibiotic mixture containing penicillin, streptomycin and neomycin (PSN, Gibco BRL), at 37 °C in a humidified incubator with 5% CO_2. For experimental study, cells were grown to 80-90 % confluence, harvested with 0.025 % trypsin (Gibco BRL) and 0.52 mM EDTA (Gibco BRL) in PBS (phosphate-buffered saline, Sigma Diagnostics) and plated at desire cell concentration and allowed to re-equilibrate for 24h before any treatment. Cells were rinsed with PBS and incubated with DMEM-containing $\mathbf{L_1H}$ and $\mathbf{L_2H}$ (10 μM, 1% DMSO) for 15 min at 37 °C. All experiments were conducted in

DMEM containing 10% FBS and 1% PSN antibiotic. The imaging system was composed of a fluorescence microscope (ZEISS Axioskop 2 plus) with an objective lens [10X].

Cell Cytotoxicity Assay

To test the cytotoxicity of **L_1H and L_2H**, MTT [*3-(4,5-dimethyl-thiazol-2-yl)-2,S-diphenyl tetrazolium bromide*] assay was performed by the reported procedure.[11] After treatments of the probe (5, 10, 25, 50, and 100 μM), 10μl of MTT solution (10mg/ml PBS) was added in each well of a 96-well culture plate and incubated continuously at 37 °C for 8 h. All mediums were removed from wells and replaced with 100μl of acidic isopropanol. The intracellular formazan crystals (blue-violet) formed were solubilized with 0.04 N acidic isopropanol and the absorbance of the solution was measured at 595 nm wavelength with a microplate reader. Values are means ± S.D. of three independent experiments. The cell cytotoxicity was calculated as percent cell cytotoxicity =100% cell viability.

Theoretical Calculation

The gradient-corrected DFT level involving the hybrid 3-parameter fit of exchange and correlation functionals of Becke (B3LYP) which includes the correlation functional of Lee, Yang, and Parr (LYP) was used. The standard split valence basis sets 6-31G(d) and 6-31G(d) were applied for other atoms. Natural population analysis (NPA) analysis (implemented in Gaussian 09 program) at B3LYP/6-31G(d) level was carried out to compute the charge on each atom.

Results and discussion

Synthesis and characterization

The organic moieties (**L_1H** and **L_2H**) were synthesized by condensing an ethanolic solution of *2-(2-aminophenyl)-benzimidazole* with benzaldehyde derivatives (for **L_1H**, *4-nitrobenzaldehyde* and for **L_2H**, *4-methoxybenzaldehyde*) in 1:1 mole ratio (**Scheme 1**). It was characterized by physico-chemico and spectroscopic tools. In addition the solid state structure of **L_1H** was confirmed by single crystal X-ray crystallography after collecting the single crystals of **L_1H** from the methanolic solutio. The molecular view of **L_1H** with atom labeling scheme is shown in **Fig. 1** which shows that **L_1H** crystallizes in the orthorhombic space group Pca21. The crystallographic data and bond parameters are tabulated in Tables 1 and 2. The bond distance of C23-N2 (1.3697 Å) is longer than that of C23-N3 (1.3220 Å) but both values are significantly shorter than that of either C4-N2 (1.4570 Å) or C4-N4 (1.4530 Å).

The peaks obtained in ^{1}H NMR spectrum of **L_1H** and **L_2H** have been assigned and these are in accordance with structural formula of the **L_1H** and **L_2H** in the solution state (**Figs. S1** and **S2**†). The ESI mass spectrum of the compound **L_1H** in methanol shows a peak at m/z 443.1480 with 100 % abundance assignable to $[M + H]^+$ (calculated value at m/z, 443.12) where M = molecular weight of **L_1H** (**Fig. S3**†). The ESI mass spectrum of the compound **L_2H** in methanol shows a peak at m/z 328.1246 with 100 % abundance assignable to $[M + H]^+$ (calculated value at m/z, 328.14) where M = molecular weight of **L_2H** (**Fig. S4,**†). IR spectra of **L_1H** and **L_2H** show the characteristic stretching of N-H and C=N bonds **(Figs.S5** and **S6**†**). L_1H** and **L_2H** undergo non-covalent hydrogen bonding interaction with HSO_4^- ions, which results in enhancement of the fluorescence intensity (**Scheme 2**).To establish the fact of the formation of the adduct with HSO_4^- ions, the species formulated as **$K[L_1H\text{-}HSO_4]$** and **$K[L_2H\text{-}HSO_4]$** were isolated in solid state from the reaction of one mole potassium hydrogen sulphate with one mole of the organic moiety (L_1H or L_2H**)** in methanol at stirring condition. The complexes are soluble in methanol, DMSO, acetonitrile. The peaks obtained in ^{1}H NMR spectrum of **$K[L_1H\text{-}HSO_4]$** and **$K[L_2H\text{-}HSO_4]$** have been assigned and these are in accordance with structural formula of the **L_1H** and **L_2H** in the solution state (**Figs. S7** and **S8**†) The ESI mass spectrum of the compound **$K[L_1H\text{-}HSO_4]$** in methanol shows a peak at m/z, 463.16 and 505.0080 (**Fig. S9**†), assignable to $[I^{2-} + 2H + Na]^+$ and $[I^{2-} + K + Na + H]^+$,where $I^{2-} = L_1^- + HSO_4^-$; and ESI mass spectrum of the **$K[L_2H\text{-}HSO_4]$** in methanol shows a peak at m/z, 447.9254 and 486.2086 (**Fig. S10**†), assignable to $[I^2 + 2H + Na]^+$ and $[I^{2-} + K + Na + H]^+$,where $I^{2-} = L_2^- + HSO_4^-$. IR spectra of **$K[L_1H\text{-}HSO_4]$** and **$K[L_2H\text{-}HSO_4]$** show the characteristic stretching of S=O at 1114 and 1111cm^{-1} respectively (**Figs. S11** and **S12**†). All these data confirm the composition of compound **$K[L_1H\text{-}HSO_4]$** and **$K[L_2H\text{-}HSO_4]$**.

^{1}HNMR titration

In order to strengthen the above pathway of bonding of HSO_4^- ions with the receptors, ^{1}H NMR titration has been performed by concomitant addition of HSO_4^- ions to the DMSO-d_6 solution of **L_1H** and **L_2H** (**Figs. S13** and **S14**, **ESI**†). Significant spectral changes of **L_1H** and **L_2H** were observed upon addition of HSO_4^- ions. In case of **L_1H** after 5 min of addition of HSO_4^- ions, the peaks due to proton of N-H^i appeared along with the peak of H^h proton at δ = 6.884-6.856 ppm (2H, m) are remarkably affected and become the peaks equivalent to one hydrogen of H^h only due to the disappear of the H^i of N-H^i. Additionally, the multiplet peaks appeared at δ = 7.361-7.337 ppm (2H, m) assignable to H^e and H$^{e'}$ protons split up as the peak for H^e shifted to downfield due to the bonding of HSO_4^- ions with H^e. In case of **L_2H** titration, the peak at 4.401 ppm due to the proton of N-H disappears after HSO_4^- addition. All other protons of **L_1H** and **L_2H** remain unaffected after interaction with HSO_4^- ions (**Tables S1**and **S2, ESI**†).

Spectral Characteristics

Emission study

L_1H and **L_2H** show emission spectrum at 485 nm in water: Ethanol (5 : 1) solvent mixture excited at 400 nm and 390 nm respectively (**Figs. S15** and **S16**†). Fluorescence quantum yields (F) were estimated by integrating the area under the fluorescence curves with the equation:

$$\phi_{sample} = \frac{OD_{standard} \times A_{sample}}{OD_{sample} \times A_{standard}} \times \phi_{standard}$$

where A is the area under the fluorescence spectral curve and OD is the optical density of the compound at the excitation wavelength. The standard used for the measurement of fluorescence quantum yield was anthracene (ϕ=0.29 in ethanol). The emission intensities of the organic molecule in presence of various concentrations of HSO_4^- ions were measured. The

fluorescence spectral properties of **L_1H** (25 μM) and **L_2H** (25 μM) were investigated in ethanol-water (1 : 5, v/v) HEPES buffer (0.1 M, pH = 7.4) at 25 °C as a function of added [HSO_4^-] (**Figs. 2a** and **2b**). **L_2H** showed a fluorescence of higher intensity at 430 nm. After addition of HSO_4^- the fluorescence intensity band shows a ratiometric enhancement at 485 nm **(Fig 2b**). Ratiometric signaling of fluorescence output at two different wavelengths plotted as a function of concentration of HSO_4^- indicates that the fluorescence intensity ratio of wave length 485 nm and 430 nm (I_{485}/I_{430}) gradually increases with increase of the concentration of HSO_4^- ions (**Fig. S17**†) and after a certain time it level up producing a sigmoid curve. The fluorescence emission band of **L_1H** at 485 nm is very weak at room temperature. Addition of HSO_4^- (25 μM) to **L_1H** (25 μM) in HEPES buffer solution at pH 7.4 afforded one hundred twenty times single point enhancement in fluorescence intensity (**Fig 2a**). In the absence of HSO_4^- anion the fluorescence intensity of **L_1H** is very low. But in presence of HSO_4^- the fluorescence intensity greatly increased due to bonding interaction between the deprotonated N^- atom (as pK_a of NH ≈ 6.9, resulted at experimental pH of the medium) of imidazole moiety with the proton of the added HSO_4^- ion. And this is also supported by the computational study of probes (**L_1H** and **L_2H**) and their corresponding adducts with HSO_4^- (**Figs. S18** and **S19**†). From this study, it also indicates that the closeness of the HSO_4^- ion with **L_1H** is in greater extent compared to **L_2H** as the theoretical bond distances of CH….O (of HSO_4^-) (2.258 Å) and N...H (of HSO_4^-) (1.898 Å) in [**L_1H-HSO_4**]$^-$ adducts are shorter than those of CH….O (of HSO_4^-) (2.371 Å) and N...H (of HSO_4) (1.958 Å) in [**L_2H-HSO_4**]$^-$ adducts. The fact due to this electronic effect plays the key role in the tuning of the fluorescence signaling from single pint response to ratiometric response.

There was almost no interference for the detection of HSO_4^- in the presence of 100 equivalent concentration of tetrabutylammonium salt of chloride, bromide, iodide and acetate; sodium salt of azide, sulphide, cyanide, dihydrogen phosphate and dihydrogen arsenate; and potassium salt of nitrate and sulphate. Job's plot analysis (**Figs. 3a** and **3b**) revealed that **L_1H** and **L_2H** both bonded with HSO_4^- ions to form the adducts in 1:1 mole ratio. The binding constant values calculated from the emission intensity data were found to be 3.25 x 10^5 $M^{-1/2}$ for **L_1H** and 1.48 x 10^5 for **L_2H** (**Figs. 4a** and **4b**) following the modified Benesi-Hildebrand equation:[12,13]

$$1/(F_x-F_0)=1/(F_{max}-F_0)+(1/K[C])(1/(F_{max}-F_0)$$

where F_0, F_x, and F_∞ are the emission intensities of organic moiety considered in the absence of HSO_4^- ions, at an intermediate HSO_4^- concentration, and at a concentration of complete interaction, respectively, and where K is the association constant and [C] is the [HSO_4^-]. The fluorescence average lifetime measurement of **L_1H** and **L_2H** in presence and absence of HSO_4^- ion in the water-ethanol (5 : 1) medium indicates the gradual increase with increase of [HSO_4^-] (**Figs. 5a** and **5b**). The average lifetimes were calculated to be 8.32 ns for only **L_1H**, 9.42 ns for the mixture of L_1H : HSO_4^- (1 : 0.5) and 10.75 ns for the mixture of L_1H : HSO_4^- at 1 : 1 mole ratio. The average lifetime for **L_2H** is 8.26 ns; for L_2H : HSO_4^- (1 : 0.5) it is 8.58 ns and in case of L_2H : HSO_4^- (1 : 1), the lifetime is 11.79 ns. The strong binding of HSO_4^- ions with organic moiety also reflected from the binding constant value. According to the equations: $\tau^{-1} = k_r + k_{nr}$ and $k_r = \Phi_f/\tau$,[14] the radiative rate constant k_r and total non-radiative rate constant k_{nr} of the organic moieties (**L_1H** , **L_2H**), **K[L_1H-HSO_4]** and **K[L_2H- HSO4]** were tabulated in Tables 3 and 4. The data suggest that the fluorescent enhancement is ascribed to the decrease of the ratio of k_{nr}/k_r from 181.40 for **L_1H** to 1.8 for **K[L_1H-HSO_4]** and from 14.4 for **L_2H** to1.0839 for **K[L_2H-HSO_4]**.

Absorption study

The UV-Vis spectrum of the **L_1H** showed the characteristic absorption bands at *ca.* 226 nm, 262 nm, 290 nm, 300 nm, and 346 nm attributable to intramolecular π–π* and n–π* transitions. In the titration by adding the solution of HSO_4^- ions to the colourless solution of **L_1H** in ethanol–water (1 : 5, v/v) HEPES buffer (0.1 M, pH 7.4) at 25 °C, the peak at 346 nm was gradually decreased and a new peak at around 390 nm was generated through an isosbestic point at 364 nm with the addition of HSO_4^- ions (**Fig. 6a**) due to the formation of complex of the receptor with HSO_4^- ion in the solution state. Similarly UV-Vis spectrum of the **L_2H** showed the characteristic absorption bands at 225 nm, 291 nm, 350 nm. In similar type of titration, addition of the solution of HSO_4^- ion to the colourless solution of **L_2H** in ethanol-water (1 : 5, v/v) HEPES buffer (0.1 M, pH 7.4) at 25 °C, the peak at 350 nm was red shifted to a new peak at 390 nm (**Fig. 6b**) through an isosbestic point at 365 nm due to the formation of adduct of **[L_2H- HSO4]**$^-$ in the solution state.

Selectivity

The fluorescence response of organic moiety towards the different anions were investigated with 100 times concentration of Cl^-, Br^-, I^-, F^-, CN^-, OAc^-, NO_3^-, S^{2-}, SO_4^{2-}, $H_2PO_4^-$, $H_2AsO_4^-$ (**Figs.S20** and **S23**). This study indicates that both **L_1H** and **L_2H** have excellent selectivity to HSO_4^- ions over other anions.

Effect of pH

The fluorescence intensity of organic moieties **L_1H** and **L_2H** were measured at various pH values in HEPES buffer (0.1 M) at 25 °C by adjusting the pH using HCl or NaOH, in presence and absence of HSO_4^- ions (**Fig 7a** and **7b**). Here, the fluorescence intensity of both organic compounds does not vary in the pH range of 5.0 - 12.0 in absence of HSO_4^- ions; but in presence of HSO_4^- ions pH independency of the fluorescence intensity of both over the pH range 5.0 to 8.0 was observed. It is also noteworthy that the fluorescence intensity of the organic moiety in presence of HSO_4^- ions is higher than those in the absence of HSO_4^- ions due to the formation of the adducts of HSO_4^- ions with the deprotonated receptors (**L_1^-** and **L_2^-** ; after the deprotonation of the nitrogen atom of –NH of the imidazole ring) through H-bonding. At the higher pH range (pH 8.0 -12.0), the gradual decrease of the fluorescence intensity is due to the decreasing formation probability of the adducts of HSO_4^- ions with the deprotonated receptors (**L_1^-** and **L_2^-**) as there is a tendency of HSO_4^- ions to be deprotonated. As a result of this observation, both probes are very effective to be used as sensors in analytical and bioanalytical studies, which were carried out at biological pH 7.4 in ethanol–water (1: 5, v/v) HEPES buffer (0.1 M) at 25 °C.

Analytical figure of merit

To calculate the detection limit the calibration curves (**Figs. 8a**

and **8b)** in the lower region (0 – 5 μM) were obtained. From the slope of the curve(s) and the standard deviation of seven replicate measurements of the zero level (σ_{zero}) the detection limit was estimated using the equation 3σ/S.[15] From this study the detection limit of $\mathbf{L_1H}$ and $\mathbf{L_2H}$ for HSO_4^- ions were calculated to be 18.8nM and 14.11 nM, respectively.

Cell Imaging

To examine the utility of the probe in biological systems, it was applied to human cervical cancer HeLa cell. Here, HSO_4^- , L_1H and L_2H were allowed to uptake by the cells of interest and the images of the cells were recorded by fluorescence microscopy following excitation at ~ 400 and 405 nm respectively (**Fig.9**). In addition, the *in vitro* study showed that 50 μM of $\mathbf{L_1H}$ and $\mathbf{L_2H}$ were not cytotoxic to cell upto 8.0 h (**Figs. S24** and **S25**). These results indicate that the probes have a potentiality for both *in vitro* and *in vivo* application as HSO_4^- sensors as well as imaging in different ways as same manner for live cell imaging can be followed instead of fixed cells. In this study, it is also observed that the clarity of the image is significantly better by employing $\mathbf{L_2H}$ than $\mathbf{L_1H}$ due to the ratiometric signaling.

Conclusion

In conclusion, two new 2-(2-aminophenyl)benzimidazol based HSO_4^- ion selective receptors ($\mathbf{L_1H}$ and $\mathbf{L_2H}$), and their 1:1 molecular adducts with HSO_4^- were synthesized and characterized by physico-chemico and spectroscopic tools along with single crystal X-ray crystallography of $\mathbf{L_1H}$ for detailed structural analysis. Both receptors ($\mathbf{L_1H}$ and $\mathbf{L_2H}$) behave as highly selective fluorescent sensor for HSO_4^- ions at biological pH in green solvent over other anions by the naked eye. Here, the newly receptors ($\mathbf{L_1H}$ and $\mathbf{L_2H}$) have the same environments to accept the guest (HSO_4^- ions), but the emission efficiency of the receptors has been tuned successfully through single point to ratiometric detection in green solvent by exploiting the substituent effects (-R effect of $–NO_2$ group and +R effect of OMe group) within the receptors. The limit of detection for HSO_4^- ions (by 3σ method) were calculated to be 18.08 nM and 14.11 nM for $\mathbf{L_1H}$ and $\mathbf{L_2H}$ respectively. Both the probes could be used as biomarkers for the detection of intracellular HSO_4^- ions in HeLa cells as both are non-cytotoxic agents but $\mathbf{L_2H}$ is better candidate compared to $\mathbf{L_1H}$ for acquiring the fluorescence image (**Fig.9**) though both have the same receptor environments for the HSO_4^- ions. From this study it may be concluded that the substituents being present in the proper position of the receptor control the mode of signaling (ratiometric or single point) of the sensor and, the ratiometric signaling is better than the single point signaling as usual.

Acknowledgments

Financial assistance from CSIR, New Delhi, India is gratefully acknowledged. M. Mukherjee wishes to thank to UGC, New Delhi, India for offering the fellowship. The authors are grateful to USIC, The University of Burdwan for the single crystal X-ray diffractometer facility under PURSE program. We sincerely acknowledge Prof. Samita Basu and Mr. Ajay Das, Chemical Science Division, SINP, Kolkata for enabling TCSPC instrument and Prof. B. Mukhopadhyay, IISER, Kolkata to record some ^{1}HNMR spectra and ESI Mass Spectra.

Notes and references

[a]*Department of Chemistry, Burdwan University, Golapbag, Burdwan-713104, West Bengal, India*
E-mail: pabitracc@yahoo.com
[b]*Department of Inorganic and Physical Chemistry, Indian Institute of Science, Bangalore, 560012, India*
[c]*Govt. college of Engineering and Leather Technology, Salt Lake Sector-III, Kolkata 9*

† Electronic Supplementary Information (ESI) available: [details of any supplementary information available should be included here]. See DOI: 10.1039/b000000x/

‡CCDC 968396 contains the supplementary crystallographic data for this paper. These data can be obtained free of charge from The Cambridge Crystallographic Data Centre *via* http://www.ccdc.cam.ac.uk/data_request/cif

(1) (a) F. P. Schmidtchen and M. Berger, *Chem. Rev*., 1997, **97**, 1609; (b) P. D. Beer, A. R. Graydon, A. O. M. Johnson and D .K. Smith, *Inorg. Chem*., 1997, **36**, 2112; (c) P. A. Gale**,** *Coord. Chem. Rev*., 2003, **240**, 191; (d) M. M. G. Antonisse and D. N. Reinhoudt, *Chem. Commun*., 1998, **4**, 443; (e) E. V. Anslyn and T. S. Snowden, *Curr. Opin. Chem. Biol.*, 1999, **3**,740; (f) P. D. Beer and P. A. Gale, *Angew. Chem. Int. Ed*., 2001, **40**, 486; (g) S. Y. Kim and J. I. Hong, *Org. Lett*., 2007**, 9**, 3109; (h) M. J. Chmielewski and J. Jurczak, *J. Eur. Chem*., 2005, **11**, 6080; (i) T. Gunnlaugsson, M. Glynn, G. M. Tocci, P.E. Kruger and F. M. feffer, *Coord. Chem. Rev*., 2006, **250**, 3094; (j) P. D. Beer and P. A. Gale, *Angew. Chem*. 2001,**113**, 502. *Angew., Chem., Int. Ed.*, 2001, **40**, 486; (k) L. Fabbrizzi, M. Licchelli, G. Rabaioli and A. Taglietti, *Coord. Chem. Rev*., 2000, **205** ,85. (l) E. J. O'Neil and B. D. Smith, *Coord. Chem. Rev*., 2006, **250**, 3068;(m) M. E. Moragues, R. Martınez-Manez and F. Sancenon, *Chem. Soc. Rev*., 2011, **40**, 2593; (n) A. F. Li, J. H. Wang, F. Wang and Y. B. Jiang, *Chem. Soc. Rev*. 2010, **39**, 3729; (o) R. M. Duke, E. B. Veale, F. M. Pfeffer, P. E. Kruger and T. Gunnlaugsson, *Chem. Soc. Rev*. 2010, **39**, 3936; (p) P. A. Gale, *Chem. Soc. Rev*. 2010, **39**, 3746; (q) P. A. Gale, Acc. *Chem. Res*., 2006, **39**, 465. (r) J. L. Sessler, P. A. Gale and W. S. Cho, in Anion Receptor Chemistry (Monographs in Supramolecular Chemistry), ed. J. F. Stoddart, RSC, Cambridge, 2006.

(2) (a) S. E. Matthews and P. D. Beer, *Supramol. Chem*. 2005, **27917**, 411;(b) Y. Michigami, Y. Kuroda, K. Ueda and Y. Yamamoto, *Anal. Chim. Acta*, 1993, **274** , 299; (c) T. Y. Joo, N. Singh, G. W. Lee and D. O. Jiang, *Tetrahedron Lett*., 2007, **48**, 8846; (d) P. Chakrabarti, *J. Mol. Biol*. 1993, **234** , 463; (e) C.Tan, Q. Wang and L. Ma, *Photochemistry and Photobiology,* 2010, **86**, 1191; (f) L. Basabe-Desmonts, D. N. Reinhoudt and M. Crego-Calama, *Integrated Analytical Systems*, 2009, **2**,81; (g) R. A. Potyrailo, V. M. Mirsky, Combinatorial Methods for Chemical and Biological Sensors, Springer, 2009.

(3) (a) A. P. Davis, D. N. Sheppard and B. D. Smith, *Chem. Soc. Rev*., 2007, **36**, 348; (b) V. Gorteau, G. Bollot, J. Mareda, A. Perez-Velasco and S. Matile, *J. Am. Chem. Soc*., 2006, **128**, 14788;(c) F. M. Ashcroft, Ion Channels and Disease Channelopathies, Academic Press, San Diego, 2000.

(4) (a) M.J. Welsh, B.W. Ramsey, F. Accurso, G.R. Cutting: Cystic fibrosis. In C.R. Scriver, A.L. Beaudet, W.S. Sly, D. Valle (eds): The Metabolic and Molecular Bases of Inherited Disease, 8th ed. New York, McGraw-Hill, 2001, pp 5121, pp 5241; (c) T. J. Jentsch, C. A. Hubner and J. C. Fuhrmann, *Nat. Cell Biol*., 2004, **6**, 1039; (d) T. J. Jentsch, T. Maritzen, A. Zdebik, *A. J. Clin. Invest*., 2005, **115**, 2039.

(5) (a) B. A. Moyer, L. H. Delmau, C. J. Fowler, A. Ruas, D. A. Bostick, J. L. Sessler, E. Katayeu, G. D. Pantos, J. M. Llinares, M. A. Hossain, S. O. Kang, K. Bowman-James , in: R.V. Eldik, K. Bowman-James, (Eds.), Advances in Inorganic Chemistry, Academic Press, New York, 2006, 175; (b) P. I. Jalava, R. O. Salonen, A. S. Pennanen, M. S. Happo, P. Penttinen, A. I. Halinen, M. Sillanpaa, R. Hillamo and M. R. Hirvonen, *Toxicol. Appl. Pharmacol*. 2008**, 229**, 146.

(6) B. Sen, M. Mukherjee, S. Pal, S.K.Mandal, M.S. Hundal, A.R. Khuda-Bukhsh and P. Chattopadhyay, ***RSC Adv.***, 2014, **4**, 15356 and references therein.

(7) (a) E. B. Veale and T. Gunnlaugsson, *Annu. Rep. Prog. Chem., Sect. B: Org. Chem*., 2010, **106**, 376; (b) M. E. Moragues, R. Martinez-Manez and F. Sancenon, *Chem. Soc. Rev*., 2011, **40**, 2593; (c) C. H. Lee, H. Miyaji, D. W. Yoon and J. L. Sessler, *Chem. Commun*., 2008**,** 24; (d) T. Gunnlaugsson, M. Glynn,. G. M. Tocci, P. E. Kruger and F. M. Pfeffer, *Coord. Chem. Rev*., 2006, **250**, 3094; (e) R. Martinez-Manez, F. Sancanon, *Chem. Rev*., 2003, **103**, 4419; (f) J. F. Callan, A. P. de Silva and D. C. Magri, *Tetrahedron*, 2005**, 61**, 8551; (g) J. Zhao, T. M. Fyles and T. D. James, *Angew. Chem., Int. Ed*. 2004**, 43** , 3461; (h) P. A. Gale, *Acc. Chem. Res*., 2006, **39**, 465; (i) S. K. Kim, D.H. Lee, J. I. Hong and J. Yoon, *Acc. Chem. Res*., 2009, **42**, 23; (j) X. Huang, Z. Guo, W. Zhu, Y. Xie and H. Tian, *Chem. Commun*., 2008**,** 5143; (k) Z. Yang, K. Zhang, F. Gong, S. Li, J. Chen, J. S. Ma, L. N. Sobenina, A. I. Mikhaleva, G. Yang and B. A.Trofimov, *Beilstein J. Org. Chem*., 2011**, 7** , 46.

(8) (a) Z. Xu, Y. Xiao, X. Qian, J. Cui and D. Cui, *Org. Lett.,* 2005, **7**, 889; (b) B. Valeur,; and I. Leray, *Coord. Chem. Rev.,* 2000, **205,** 3; (c) S. Sen, S. Sarkar,B. Chattopadhyay, A. Moirangthem, A. Basu, K. Dhara and P. Chattopadhyay, *Analyst*, 2012, **137**, 3335.

(9) A. Altomare, G.Cascarano, C. Giacovazzo and A. Guagliardi, *J. Appl. Crystallogr*., 1993, **26**, 343.

(10) L.J. Farrugia, *J. Appl. Cryst*., 1999, **32**, 837.

(11) (a) S. Banerjee, P. Prasad, A. Hussain, I. Khan, P. Kondaiah and A.R. Chakravarty, *Chem. Commun.,* 2012, **48**, 7702 (b) T. Mosmann, *J. Immunol. Methods*., 1983, **65**, 55.

(12) A. Mallick and N. Chattopadhyay, *Photochem. Photobiol*., 2005, **81**, 419.

(13) H. A. Benesi, J. H. Hildebrand, *J. Am. Chem. Soc*., 1949, **71**, 2703.

(14) N. J. Turro, *Modern Molecular Photochemistry*, Benjamin/ Cummings Publishing Co., Inc., Menlo Park, CA, 1978, p. 246.

(15) (a) A. Hakonen, *Anal. Chem*., 2009, **81**, 4555; (b) S. Pal, B. Sen, M. Mukherjee, K. Dhara, E. Zangrando, S.K. Mandal, A.R. Khuda-Bukhsh, and P. Chattopadhyay, Analyst, 2014, **139**, 1628.

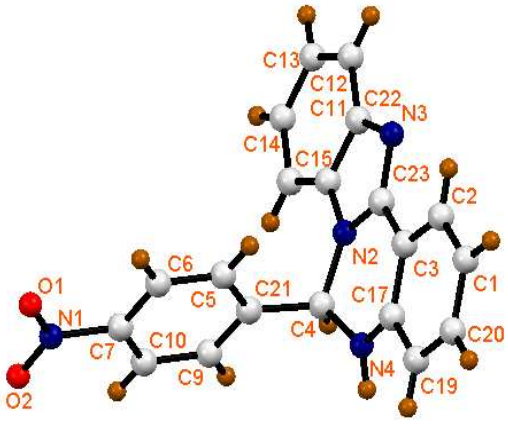

Fig. 1 A molecular view with atom numbering scheme of $\mathbf{L_1H}$

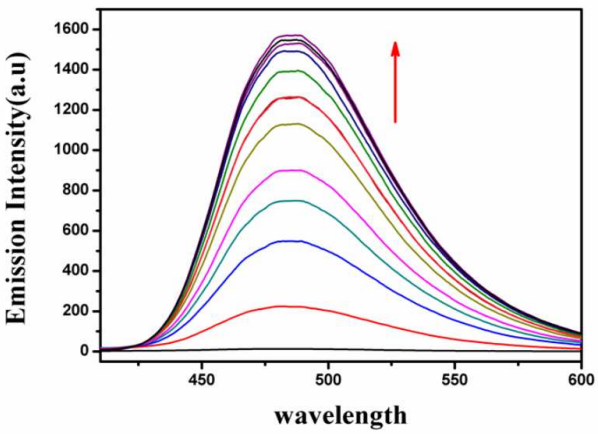

Fig. 2a Fluorescence spectra of $\mathbf{L_1H}$ (25 μM) as a function of externally added HSO_4^- [0-30 μM] in ethanol-water (1 : 5, v/v) HEPES buffer (0.1 M, pH = 7.4) at 25 °C [λ_{em} = 485 nm, λ_{ex} = 400 nm].

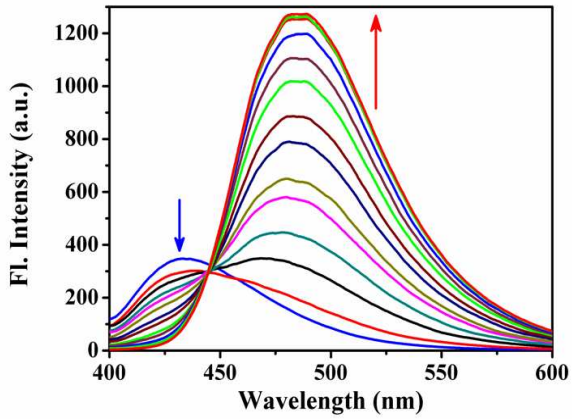

Fig. 2b Fluorescence spectra of $\mathbf{L_2H}$ (25 μM) as a function of externally added HSO_4^- [0–30 μM] in ethanol–water (1 : 5, v/v) HEPES buffer (0.1 M, pH = 7.4) at 25 °C [λ_{em}: 485 nm, λ_{ex} = 390 nm].

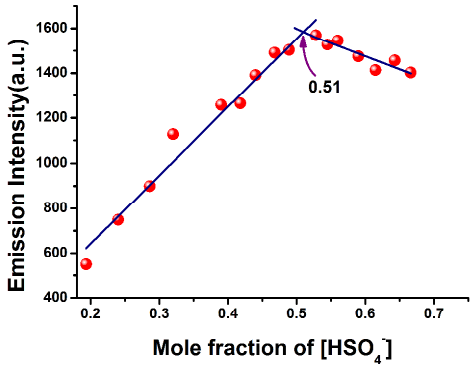

Fig. 3a Job's plot of $\mathbf{L_1H}$ showing maxima at 1:1

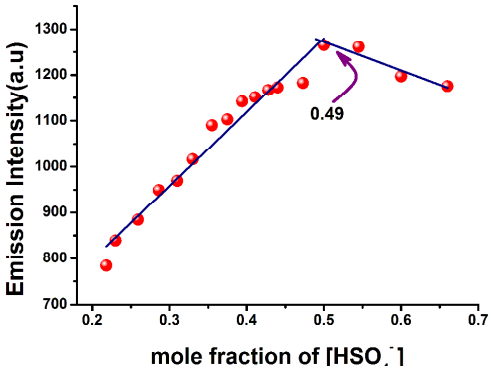

Fig. 3b Job's plot of L_2H showing maxima at 1:1

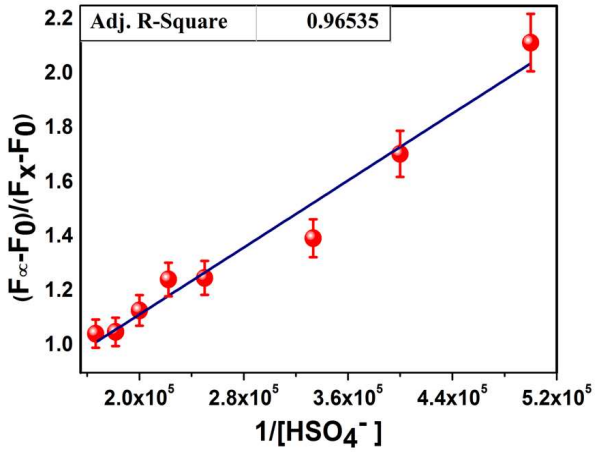

Fig. 4a Binding constant (K) value of 3.25 X 10^5 M^{-1} for L_1H determined from the intercept/slope of the plots.

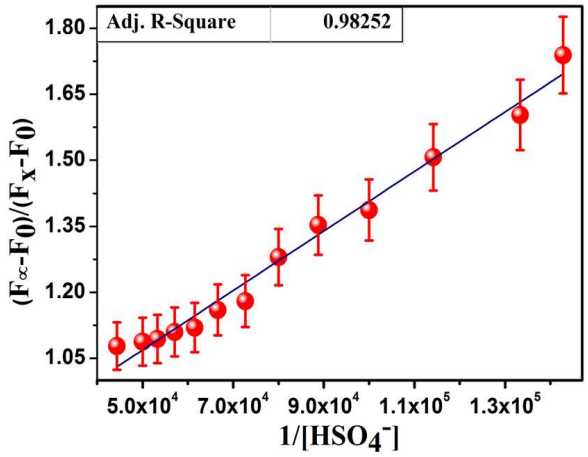

Fig. 4b Binding constant (K) value of 1.48 X 10^5 M^{-1} for L_2H determined from the intercept/slope of the plots.

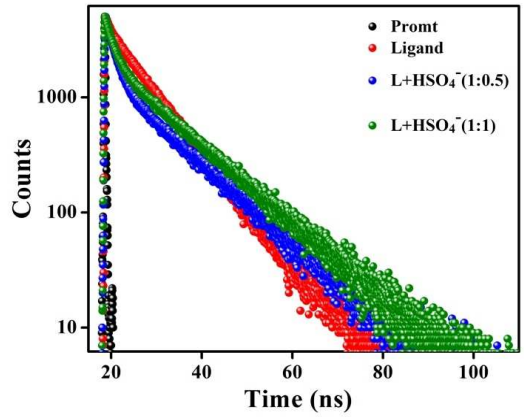

Fig. 5a Time-resolved fluorescence decay of L_1H (10 mM) in the absence and presence of added HSO_4^- ions (5 mM and 10 mM) (at λ_{ex} = 400 nm) in 100 mM HEPES buffer (ethanol/ water: 1/5, v/v) [λ_{em} = 485 nm].

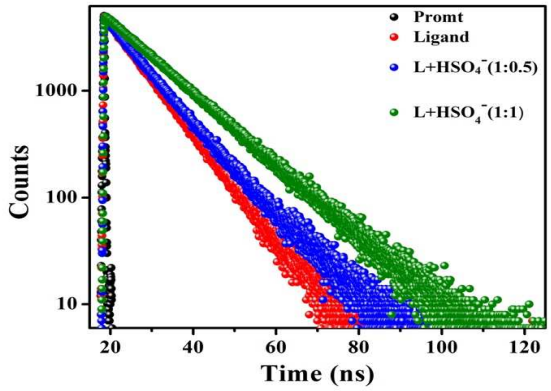

Fig. 5b Time-resolved fluorescence decay of L_2H (10 mM) in the absence and presence of added HSO_4^- ions (5 mM and 10 mM) (at λ_{ex} = 390 nm) in 100 mM HEPES buffer (ethanol/ water: 1/5, v/v) [λ_{em}: 485 nm].

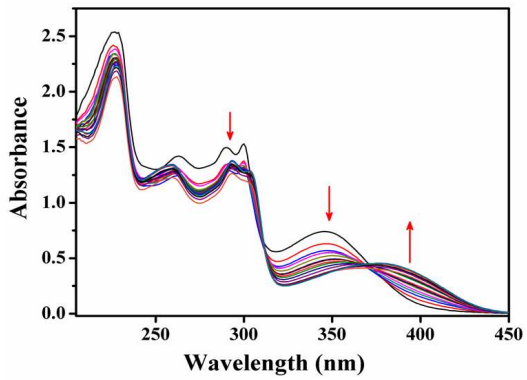

Fig. 6a Changes in the absorption spectra of L_1H (25 μM) upon addition of 0–30 μM of HSO_4^- in ethanol–water (1 : 5, v/v) HEPES buffer (0.1 M, pH 7.4) at 25 °C.

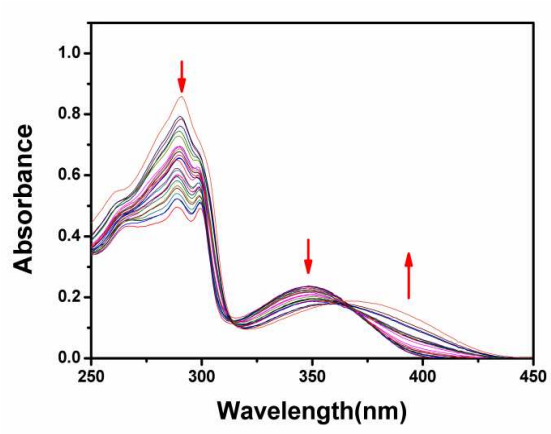

Fig. 6b Changes in the absorption spectra of $\mathbf{L_2H}$ (25 μM) upon addition of 0-30 μM of HSO_4^- in ethanol–water (1 : 5, v/v) HEPES buffer (0.1 M, pH 7.4) at 25 °C.

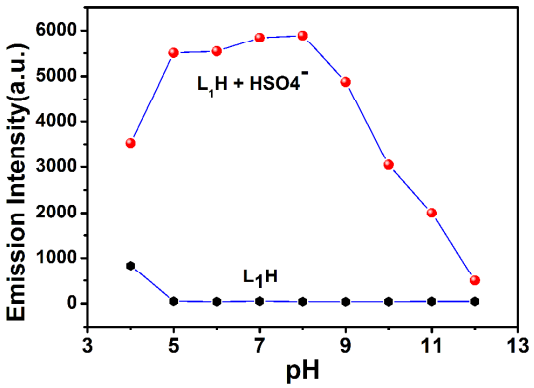

Fig. 7a Fluorescence response to pH of $\mathbf{L_1H}$ (25 μM) in absence and in presence of HSO_4^- (one equivalent) at different pH in 100 mM HEPES buffer (ethanol/ water: 1/5) at 25 °C.

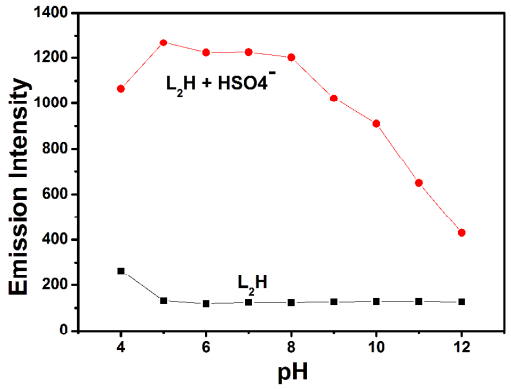

Fig. 7b Fluorescence response to pH of $\mathbf{L_2H}$ (25 μM) in absence and in presence of HSO_4^- (one equivalent) at different pH in 100 mM HEPES buffer (ethanol/ water: 1/5) at 25 °C.

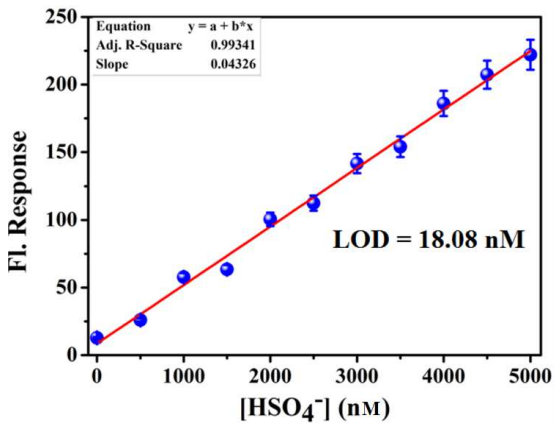

Fig. 8a Calibration curve for the nanomolar range, with error bars for calculating the LOD of HSO_4^- by $\mathbf{L_1H}$ in 100 mM HEPES buffer (ethanol/ water: 1/5) at 25 °C.

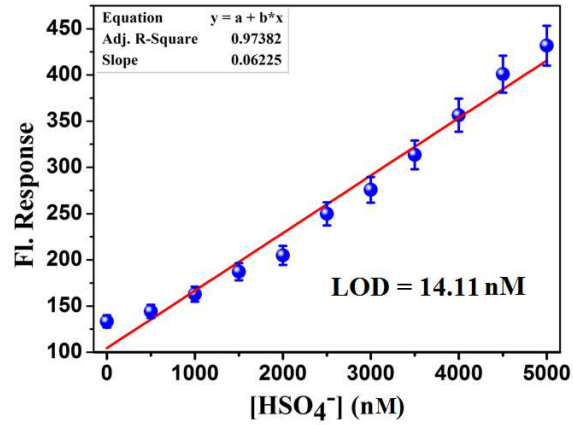

Fig. 8b Calibration curve for the nanomolar range, with error bars for calculating the LOD of HSO_4^- by $\mathbf{L_2H}$ in 100 mM HEPES buffer (ethanol/ water: 1/5) at 25 °C.

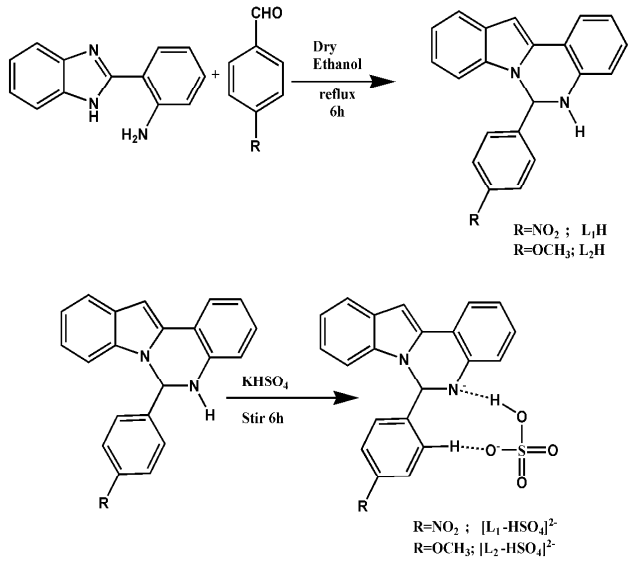

Scheme1 Schematic representation of synthesis of the probes $\mathbf{L_1H}$ and $\mathbf{L_2H}$ and their corresponding complexes.

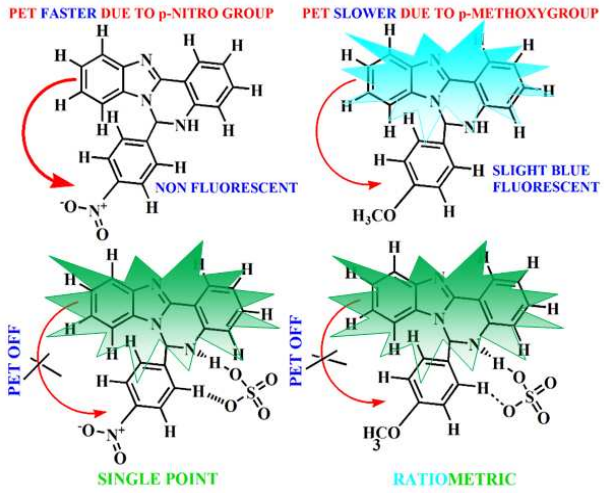

Scheme 2 Schematic representation of the plausible mechanism of hydrogen sulfate sensing.

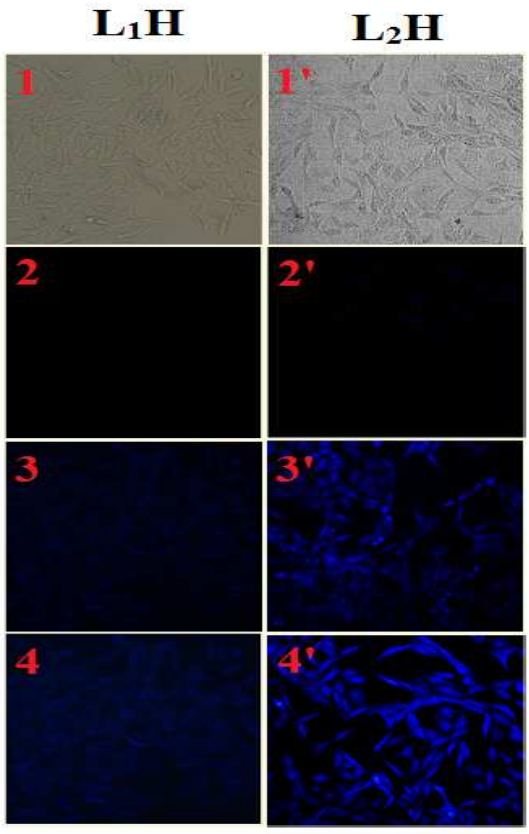

Fig.9 Phase contrast (**1, 1′**) and fluorescence images of HeLa cells after incubation with LH in presence of hydrogen sulphate ions (**2, 2′**) 0 μM, (**3, 3′**) 5 μM and (**4, 4′**) 10 μM respectively with HSO_4^- for 30 min at 37 °C.

Table 1 Crystal data and details of refinements for **L_1H**

Empirical Formula	$C_{20}H_{15}N_4O_2$
Formula Weight	343.36
Crystal system	orthorhombic
Space group	Pca21
a (Å)	12.0792(5)
b (Å)	9.1171(4)
c (Å)	15.1341(7)
$\alpha = \beta = \gamma$	90^O
Volume (Å^3)	1666.68(13)
Temperature (K)	296(2)
Z	4
ρ_{calc} (g/cm^3)	1.368
μ (mm^{-1})	0.092
F(000)	716
θ range (deg)	2.80 - 26.78
Reflections collected	26495
Reflections independent	3542
Final R indices [$I > 2\sigma(I)$]	3202
R indices (all data)	0.0302
Goodness-of-fit on F^2	1.033

Table 2 Selected bond distances (Å) and bond angles (°) for L_1H

Bond length (Å)	
C22-N3	1.389(2)
C23-N3	1.3220(18)
C23-N2	1.3697(19)
N2-C11	1.386(2)
N2-C4	1.4570(17)
C7-N1	1.471(2)
Bond angles (^{0})	
N3 - C23 - N2	112.68(13)
N3 - C23- C3	128.21(13)
N2 - C23 - C3	119.10(12)
C23 - N2 - C11	107.34(11)
C23 - N2 - C4	126.13(13)
C11 - N2 - C4	126.27(13)
N3 - C22 - C12	130.12(14)
N3 - C22 - C11	110.30(13)
N4 - C4 - N2	108.20(12)
N4 - C4 - C21	112.33(12)
N2 - C4 - C21	111.87(11)

Graphical Abstract

Substituent effect on tuning of fluorescence signaling of the cell permeable HSO_4^- receptors through single point to ratiometric response in green solvent has been explored taking two newly designed HSO_4^- ion selective receptors with structural similarity except one difference of the substituent in the *para* position to the phenyl ring attached to the the quinazoline ring (*para-nitro* in $\mathbf{L_1H}$ and *para-methoxy* in $\mathbf{L_2H}$) by thorough analytical and biological studies.